JACS
JOURNAL OF THE AMERICAN CHEMICAL SOCIETY
Article
pubs.acs.org/JACS

Cyclic Denaturation and Renaturation of Double-Stranded DNA by Redox-State Switching of DNA Intercalators

Shahida N. Syed,[†] Holger Schulze,[†] Daniel Macdonald,[†] Jason Crain,[‡,⊥] Andrew R. Mount,[§] and Till T. Bachmann*[,†]

[†]Division of Pathway Medicine, School of Biomedical Sciences, The University of Edinburgh, Chancellor's Building, Little France Crescent, Edinburgh EH16 4SB, Scotland, U.K.

[‡]School of Physics and Astronomy, The University of Edinburgh, The King's Buildings, West Mains Road, Edinburgh EH9 3JZ, Scotland, U.K.

[⊥]National Physics Laboratory, Hampton Road, Teddington, Middlesex TW11 0LW, England, U.K.

[§]EastCHEM, School of Chemistry, The University of Edinburgh, Joseph Black Building, West Mains Road, Edinburgh EH9 3JJ, Scotland, U.K.

Supporting Information

ABSTRACT: Hybridization of complementary nucleic acid strands is fundamental to nearly all molecular bioanalytical methods ranging from polymerase chain reaction and DNA biosensors to next generation sequencing. For nucleic acid amplification methods, controlled DNA denaturation and renaturation is particularly essential and achieved by cycling elevated temperatures. Although this is by far the most used technique, the management of rapid temperature changes requires bulky instrumentation and intense power supply. These factors so far precluded the development of true point-of-care tests for molecular diagnostics. To overcome this limitation we explored the possibility of using electrochemical means to control reversible DNA hybridization by using the electroactive intercalator daunomycin (DM). We show that redox-state switching of DM altered its properties from DNA binding to nonbinding, under otherwise constant conditions, and thus altered the thermodynamic stability of duplex DNA. The operational principle was demonstrated using complementary synthetic 20mer and 40mer DNA oligonucleotides. Absorbance-based melting curve analysis revealed significantly higher melting temperatures for DNA in the presence of oxidized compared to chemically reduced DM. This difference was exploited to drive cyclic electrochemically controlled denaturation and renaturation. Analysis with *in situ* UV−vis and circular dichroism spectroelectrochemistry, as two independent techniques, indicated that up to 80% of the DNA was reversibly hybridized. This remarkable demonstration of electrochemical control of five cycles of DNA denaturation and renaturation, under otherwise constant conditions, could have wide-ranging implications for the future development of miniaturized analytical systems for molecular diagnostics and beyond.

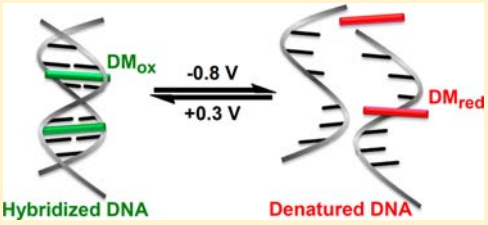

INTRODUCTION

Denaturation and renaturation, the reversible interconversion between double-stranded DNA (dsDNA) and single-stranded DNA (ssDNA), is crucial in many biological processes such as DNA replication. These processes, also termed DNA melting and hybridization, involve the breakage/formation of hydrogen bonds, as well as $\pi-\pi$ and van der Waals interactions involved in base stacking.[1,2] While the renaturation of two ssDNA strands is thermodynamically favorable under ambient conditions, denaturation of dsDNA is unfavorable and does not occur spontaneously. However, both processes can be controlled for example by temperature, altering the pH or ionic strength, and different chemical agents.[3−7] DNA denaturation/renaturation also plays an integral role in many methods and applications targeting *in vitro* diagnostics, such as biosensors[8,9] and DNA microarrays[10,11] or any nucleic acid amplification method (e.g., the polymerase chain reaction or ligase chain reaction)[12−14] and next generation sequencing.[15] Thus, there is a prevailing interest in further understanding and controlling this reversible process.[16,17] Many *in vitro* diagnostic platforms today require expensive, high-energy consuming, benchtop sized instruments in centralized laboratories which struggle to meet the requirements of the increasing demands on decentralized testing. The interest in making diagnostics cheaper, faster and user-friendly has generated a focus on integration of laboratory operations, such as nucleic acid amplification or sample preparation, into miniaturized and fully automated lab-on-a-chip devices or micro total analysis systems (μTAS).[13,18−20] This has brought the possibility of portable testing within reach.[21,22] However, most nucleic-acid based diagnostic techniques rely on thermal control for the reversible hybridization of nucleic acids. This poses several challenges for the integration into μTAS, such as bulk thermal cycling with

Received: December 5, 2012
Published: March 6, 2013

   dx.doi.org/10.1021/ja311873t | J. Am. Chem. Soc. 2013, 135, 5399−5407

Scheme 1. Reversible Reduction and Oxidation of Daunomycin As Postulated To Be Involved in the Electrochemical Control of DNA Hybridization in This Study

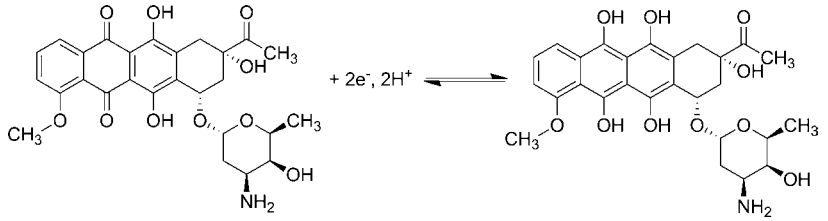

expensive heating and cooling elements and issues with evaporation and bubble formation.[13,19,23] Consequently, the implementation of alternative ways to control reversible hybridization of nucleic acids may be a key success factor in the development of portable nucleic acid-based diagnostics. Owing to properties such as high sensitivity, fast response and low cost, electrochemical-based sensing is an active area of research for use in the development of point-of-care tests.[8] Indeed, it furthermore enables simpler operations suitable for miniaturization and integration into μTAS.[24,25] Hence, replacing thermal control of reversible DNA hybridization by isothermal electrochemical means is a highly attractive opportunity to achieve miniaturized analytical systems which could be integrated into μTAS to enable truly decentralized diagnostics.

Wang et al. recently demonstrated four cycles of denaturation/renaturation of 290 base-pairs long DNA fragments via electrochemically driven pH change. The cycling was obtained by changing the bulk pH between 5.2 and 11.4 through the application of an overall cell current, and the same current of reverse polarity to inject and remove HCl.[6] In contrast, Asanuma and co-workers investigated photoregulation by covalently attaching azobenzene units on short DNA oligonucleotides. The azobenzene units were reversibly isomerized from planar *trans* to nonplanar *cis* form upon the irradiation of UV or visible light facilitating denaturation/renaturation.[26] Others have explored reversible control through photoregulation of non-covalently binding DNA molecular glue,[17] or electronic control using radio frequency magnetic field to induce heating and subsequent cooling for the denaturation/renaturation of DNA-modified gold nanoparticles.[27]

Despite many approaches to replace thermal control of reversible DNA hybridization, no method has been presented which enables fast, isothermal electrochemical control that does not require dramatic change of solution conditions or modification or immobilization of DNA nucleotides. To overcome these limitations, we propose the use of DNA intercalators. These molecules are organic, planar and frequently electroactive. They contain aromatic moieties that interact with DNA through intercalation. This process is characterized by the perpendicular insertion of the molecule between stacked base-pairs causing conformational changes of the double helix, such as unwinding, lengthening and increasing rigidity.[28] While intercalators mainly stabilize dsDNA through base stacking, further stabilization can be achieved by interactions of side groups with base-pairs, backbone, and the surface of the double helix. These interactions comprise H-bonding, van der Waals, and electrostatic interactions.[28] The electroactivity of many intercalators such as daunomycin (DM) has been vastly exploited in electrochemical detection of nucleic acids.[8,29−31] DM is an anthracycline antibiotic and consists of an aglycone unit, which intercalates into dsDNA, and a sugar ring which binds in the minor groove.[32] Crystallographic studies by Quigley et al. revealed that one DM binds per every three base-pairs and is stabilized by three H-bonds as well as several van der Waals interactions.[32] The electroactive aglycone unit contains an oxidizable hydroquinone ring and a reducible quinone ring. In aqueous solutions, DM can undergo a reversible $2e^-$ reduction of the quinone to a full hydroquinone as depicted in Scheme 1.[33] The oxidized form of DM has been found to stabilize and increase the melting temperature (T_M) of DNA by up to 30 °C.[34] Whereas the effect of oxidized DM on DNA has been well-documented in terms of structural studies and binding properties[34−37] similar systematic studies regarding the impact of reduced DM on DNA have not been published.

For this study, we hypothesized that oxidized and reduced form of DM bind differently to dsDNA and thus affect the relative stability of ds and ssDNA expressed by an altered association constant. Accordingly, redox conversion of DM opens the prospect of isothermal reversible control of DNA hybridization. This proof-of-principle paper demonstrates that electrochemical redox cycling of the DM oxidation state leads to cycles of DNA denaturation and renaturation, thereby circumventing the need for thermal control of this process. This was confirmed in independent experiments using *in situ* UV−vis and circular dichroism (CD) spectroelectrochemistry.

EXPERIMENTAL SECTION

All solutions were prepared or diluted with ultrapure water (Milli-Q Synthesis, resistance = 18.4 MΩ cm, Millipore Corp., Bedford, MA, USA). Experiments were conducted in saline−sodium citrate buffer [1× SSC (0.15 M NaCl with 15 mM trisodium citrate), pH 7 adjusted with HCl] from Fisher Scientific (Loughborough, UK) and diluted further as required. Analytical grade ethanol, concentrated nitric acid (HNO_3) and 0.1 M sulfuric acid (H_2SO_4) were used for cleaning and purchased from VWR Laboratories (Lutterworth, UK). Complementary 20mer and 40mer oligonucleotides were purchased from Metabion (Martinsried, Germany). Stock solutions were prepared by dissolving lyophilized DNA in water and stored at −20 °C. Concentrations were determined using NanoDrop ND-1000 UV−vis spectrophotometer (NanoDrop Technologies, Wilmington, DE, USA). Daunomycin [DM, (8*S*,10*S*)-8-acetyl-10-[(3-amino-2,3,6-trideoxy-α-L-lyxo-hexopyransoyl)oxy]-7,8,9,10-tetrahydro-6,8,11-trihydroxy-1-methoxy-5,12-naphthacenedione hydrochloride; $\lambda_{ex/em}$ = 480/592 nm, $\varepsilon_{480\ nm}$ = 11 500 M^{-1} cm^{-1}] was purchased from Tocris Bioscience (Bristol, UK). A stock solution was prepared in water and aliquots were stored in dark at −80 °C. Diluted DM was freshly prepared for each experiment. Electrochemical experiments were performed with a three-electrode setup in a thin-layer spectroelectrochemical quartz cuvette (path length 0.5 mm). A Pt gauze working electrode (WE) was used with a Pt wire counter electrode (CE) and a single fritted Ag/AgCl (3 M NaCl) reference electrode (RE) from IJ Cambria Scientific (Carms, UK). Spectrophotometric experiments were conducted on an Agilent Cary 60 UV−vis spectrophotometer equipped with a Varian Cary Peltier Accessory for temperature control

dx.doi.org/10.1021/ja311873t | *J. Am. Chem. Soc.* 2013, 135, 5399−5407

(Agilent Technologies, Wokingham, UK). A Digitron Model 3900 thermocouple (RS Components, Corby, UK) was used to monitor the temperature inside the cuvette. A PalmSens hand-held potentiostat/galvanostat (PalmSens, Houten, Netherlands) was used for electrochemical experiments, while a Jasco J-810 circular dichroism spectropolarimeter equipped with a Peltier thermoelectric type temperature controller (Jasco International, Great Dunmow, UK) was employed for CD experiments.

Sample Preparation. DNA experiments were carried out with a 1:1 mixture of complementary DNA oligonucleotides (20mer or 40mer) at a base-pair (bp) concentration of 200 μM in 0.036× SSC (5.9 mM Na^+) or 0.1× SSC (16.5 mM Na^+) buffer (pH 7). For dsDNA, oligonucleotides were hybridized by initial denaturation for 5 min at 95 °C while shaking at 450 rpm using a Thermomixer comfort (Eppendorf, Hamburg, Germany), followed by cooling down to room temperature over 3.5 h to ensure complete duplex formation. Samples were stored at +4 °C and used within a week. For DNA with DM, intercalation was carried out before the experiment by adding DM to a final concentration of 100 μM (molar ratio of dsDNA-bp:DM = 2:1), and then the mixture was incubated for 10 min at 25 °C, 450 rpm, protected from light. The solution was degassed for 2.5 min with argon and then overlaid for 1 min to remove oxygen. Next, 300 μL of the sample was added to the cuvette followed by electrode assembly (if applied). To prevent evaporation, the sample was overlaid with mineral oil (Biomérieux, Hapmshire, UK) and the cuvette was sealed with Teflon tape and parafilm. Prior to use, the cuvette was cleaned with ethanol and water and then finally dried with compressed air.

Cleaning of Electrodes. The Pt gauze WE and Pt wire CE were immersed in concentrated HNO_3 for 5 min at room temperature followed by rinsing with water and drying with a stream of N_2. The WE was electrochemically cleaned in 0.1 M H_2SO_4 using cyclic voltammetry. First 1.4 to −0.2 V was cycled 40 times, followed by 10 times cycling of 1.14 to −0.24 V, at 50 mV/s. Electrodes were finally rinsed with water and dried with a stream of N_2 before use.

DNA Melting Studies. Melting curves were acquired for dsDNA with and without oxidized/chemically reduced DM. Samples were prepared as above, while chemical reduction of DM took place after intercalation. Reduction was achieved by adding sodium borohydride ($NaBH_4$, Sigma Aldrich, Poole, UK) in excess to a final concentration of 5 mM and incubated at 25 °C, 450 rpm, for 60 min. After baseline correction with the appropriate buffer, renaturation followed by denaturation was recorded by scanning the wavelength range 800−200 nm at 4800 nm/min (bandwidth 2 nm, interval 1 nm) between 25 and 95 °C (depending on sample) at 1 °C/min. Melting curves were plotted of the absorbance at 260 nm ($A_{260\,nm}$) as a function of temperature (T). For calculation of T_M and thermodynamic parameters a two-state model, where the DNA is either single-stranded or double-stranded, was assumed.[38] Furthermore, assuming the temperature-independence of $\Delta H°$ and $\Delta S°$, the parameters could be derived from the van't Hoff plot of $\ln(K_a)$ versus $1/T$ (K^{-1}) using the thermodynamic relationship in eq 1.[3,39] The hyperchromic shift H was calculated using eq 2, where $A_{T,upper}$ and $A_{T,lower}$ are the absorbances at the upper and lower temperature, respectively.

$$\Delta G° = -RT\ln(K_a) = \Delta H° - T\Delta S° \quad (1)$$

$$H_{260\,nm} = (A_{T,upper} - A_{T,lower})/A_{T,lower} \times 100 \quad (2)$$

Cyclic Voltammetry. The redox behavior of 100 μM DM in 0.036× SSC (5.9 mM Na^+) was investigated by scanning the potential range from 0.3 to −0.8 V vs Ag/AgCl RE 5 times at room temperature with a scan rate of 5 mV/s. Prior measurement, the electrodes were cleaned as described above and the solution was degassed for 2.5 min with argon and then overlaid for 1 min.

Switch Experiments with *in Situ* UV−Vis Spectroelectrochemistry. dsDNA with DM was prepared as above. After baseline correction with the appropriate buffer, 300 μL of sample was added to the cuvette, electrodes were assembled, and finally the cuvette was sealed. A spectrum was first recorded at 25 and 58−65 °C without applying a potential to ensure that the dsDNA was not denatured at the selected working temperature (T_{work}; see Table 1). This was followed by applying successive reduction (−0.8 V) and oxidation potentials (+0.3 V) at T_{work} five times and recording spectra after 60 s of potential application. The spectra were collected within 10 s, to minimize risk of DNA damage through UV radiation, by scanning the wavelength range from 800−200 nm at 4800 nm/min (bandwidth 2 nm, interval 1 nm). The current was recorded continuously. A final reduction/oxidation potential sequence was then conducted at the respective heat denaturation temperature, 85−95 °C (see Table 1), as an internal control. At this temperature the DNA was expected to be denatured regardless of the redox state of DM. To confirm that the dsDNA remained intact, a final spectroscopic scan was performed at 25 °C without applying a potential. As controls, the same experiment was carried out omitting either DNA or DM, or performing the experiment at 25 °C where the DNA is expected to be hybridized. Samples and controls were measured at least three times. The exclusive switching effect from DNA was calculated using

$$A^{DNA}_{260\,nm}(T_{work}) = A^{DNA+DM}_{260\,nm}(T_{work}) - \bar{A}^{DM}_{260\,nm}(T_{work}) \quad (3)$$

where $A^{DNA+DM}_{260\,nm}(T_{work})$ and $\bar{A}^{DM}_{260\,nm}(T_{work})$ are the absorbance observed for DNA in the presence of DM at T_{work} and the mean absorbance obtained from switching DM alone at T_{work}, respectively. The exclusive absorbance from DNA was then used to calculate the hyperchromic shift using

$$H_{260\,nm} = (A^{DNA}_{red} - A^{DNA}_{ox})/A^{DNA}_{ox} \times 100 \quad (4)$$

where A^{DNA}_{red} and A^{DNA}_{ox} are the exclusive absorbance of DNA at 260 nm upon applying a reduction and oxidation potential, respectively.

RESULTS AND DISCUSSION

The aim of this study was to demonstrate the electrochemical control of cyclic DNA denaturation and renaturation. A model system was chosen based on the objective to establish starting conditions in which the DNA strands would be renatured. Then, by applying an electrochemical trigger (reduction of electroactive intercalator DM) the hybridized DNA strands would be transferred into a condition in which the thermodynamic stability of the double helix decreased and dissociated into single strands. Upon reversion of the electrochemical trigger (oxidation of electroactive intercalator DM) the single strands would renature. This system was realized for 20mer and 40mer dsDNA oligonucleotides as well as for two different salt concentration, low (5.9 mM Na^+) and high (16.5 mM Na^+). Initial assessment of the effect of DM on DNA hybridization was made by recording DNA melting curves. Together with establishing the redox behavior of DM, the working conditions, such as working temperature and redox potentials for switching, were determined for the electrochemical switch experiments. Thereafter, cycles of electrochemically controlled DNA denaturation and renaturation, through the switching of the DM redox state, were confirmed using *in situ* UV−vis and CD spectroelectrochemistry.

Influence of Oxidized and Reduced DM on DNA. To study the influence of DM, melting curves of DNA in the absence and presence of oxidized/reduced DM were recorded. As it was not desirable to expose the sample with a reduction potential for >3 h DM was reduced chemically in these experiments using $NaBH_4$ in excess. Figure 1 shows renaturation curves for 20mer DNA in SSC buffer (5.9 mM Na^+) as typical examples. For clear visualization of differences in T_M, the curves were normalized to the maximum value between 0% and 100%. Results for 40mer and 20mer DNA in SSC buffer (5.9 and 16.5 mM Na^+, respectively) are found in Figure S1 (Supporting Information). Table 1 summarizes the T_M values and hyperchromic shifts. T_M of DNA increased significantly in the presence of oxidized DM by up to 32.9 °C,

dx.doi.org/10.1021/ja311873t | J. Am. Chem. Soc. 2013, 135, 5399−5407

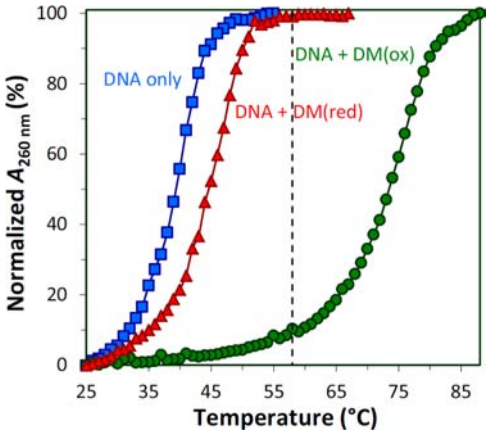

Figure 1. DNA melting curves of complementary 20mer DNA oligonucleotides in the absence and presence of oxidized and chemically reduced DM (molar ratio 2:1). Recorded at 1 °C/min in SSC buffer (5.9 mM Na^+). Dashed line represents the selected working temperature for the electrochemical switch experiments. Unlike reduced DM, oxidized DM increases T_M of DNA significantly.

which corresponds well with the findings of Chaires et al.[34] In contrast, reduced DM only caused a slight increase in T_M. The mean difference in T_M between DNA in the presence of oxidized and reduced DM for all investigated conditions was found to be 26.3 ± 1.9 °C. The working temperature (T_{work}) and the heat denaturation temperature for the electrochemical switch experiments were selected at the point where 0% or 100% of the DNA was in a denatured state in the presence of oxidized DM and reduced DM, respectively. The dashed line in Figure 1 represents the selected working temperature for 20mer DNA in SSC buffer (5.9 mM Na^+), and a summary for all conditions is in found in Table 1.

The majority of the existing literature on DM binding to DNA has focused on the characterization of the thermodynamic profile of the drug-binding action. However, the focus of the present study lies within understanding the effect of the intercalator on the thermodynamics of the hybridization/renaturation of DNA. Hence, the thermodynamic parameters of DNA for all three investigated conditions were calculated on the basis of van't Hoff analysis (see Table 2) to provide an initial understanding of the effects on DNA caused by DM. These experimentally determined parameters for 20mer DNA alone corresponded well with predicted values from IDT Biophysic's DNA thermodynamics and hybridization calculator[40] (see Table S2). Furthermore, similar enthalpy, entropy and Gibb's free energy values for 20mer DNA in the presence of oxidized DM were observed by Belozerova and Levicky[41] for the renaturation of short DNA strands in the presence of the minor groove binding molecule netropsin. However, discrepancies were found for the 40mer DNA alone between the calculated and predicted value suggesting it may not be following the two-state model assumed and thus needs further evaluation.[3] Nevertheless, it is apparent that two different redox states of DM bind and affect the stability of the double helix differently. $\Delta G°$ was found to be more negative for DNA in the presence of oxidized DM while reduced DM displayed a $\Delta G°$ almost equal to DNA alone. Accordingly, oxidized DM dramatically increased the observed association constant K_a by 4 orders of magnitude (evaluated at T_{work}) for DNA compared to the reduced form. In accordance with our hypothesis this confirmed that, at the selected working temperature, oxidized DM stabilized the DNA while reduced DM did not.

Electrochemical Characterization of Daunomycin. The redox properties of DM were investigated by means of cyclic voltammetry and *in situ* UV–vis spectroelectrochemistry. For the purpose of the method in this study, only reduction to a full hydroquinone was required (see Scheme 1). Figure S2 displays a fully reversible voltammogram with an oxidation peak potential E_{pc} = −0.43 V and a reduction peak potential E_{pa} = −0.59 V. E_{pa} was consistent with previously published values for a $2e^-$ reduction of the anthracycline quinone ring,[36,42] whereas the differing E_{pc}, and hence the large peak separation (ΔE_p = 154 mV), is more likely an effect of the ohmic drop due to the design of the spectroelectrochemical cell.[43] The scanned potentials only displayed one set of redox peaks substantiating that only reduction of the quinone was taking place. The mechanism sequence of DM reduction has been established to involve two consecutive one e^- reductions through the formation of a semiquinone and finally hydroquinone.[44,45] However, it has likewise been established that the reaction equilibrium of the semiquinone formation favors the quinone or the hydroquinone, rendering the intermediate semiquinone unstable.[46] The reversible formation of the hydroquinone was confirmed with *in situ* UV–vis spectroelectrochemistry. To ensure complete oxidation and reduction of DM in the electrochemical switch experiments, −0.8 and +0.3 V were chosen as reduction and oxidation potential. Figure 2 depicts typical absorption changes of DM upon cycling −0.8 and +0.3 V five times at 58 °C. When no potential was applied (at T_{start}, T_{work}, and T_{finish}), DM remained oxidized with characteristic peaks[47] at 233, 253, and 480 nm. Upon reduction of DM at −0.8 V, characteristic peaks[45] for the $2e^-$ reduction to a full hydroquinone appeared at 262 and 435 nm. A continuous decrease in absorbance was however observed per reduction, whereas it slightly increased again at the heat denaturation temperature 85 °C. Upon re-oxidation at +0.3 V, the characteristic peaks for oxidized DM re-appeared. Although the observed peaks were constant, they were less pronounced and the third peak at 500 nm was slightly shifted, which was not the case for the re-oxidation at 85 °C. The continuous decrease in absorbance for reduced DM, and the less pronounced

Table 1. Values for T_M and Hypochromic Shifts (H) of DNA with Oxidized or Chemically Reduced DM[a]

	DNA		DNA with DM_{ox}		DNA with DM_{red}			
conditions	T_M (°C)	H (%)	T_M (°C)	H (%)	T_M (°C)	H (%)	T_{work} (°C)	heat denaturation T (°C)
20mer, 5.9 mM Na^+	40.1	20.6	72.9	34.0	46.1	15.1	58.0	85.0
40mer, 5.9 mM Na^+	51.0[b]	24.6	86.0[b]	34.6	58.0[b]	14.3	65.0	95.0
20mer, 16.5 mM Na^+	49.6	22.6	76.6	37.4	52.4	10.1	60.0	90.0

[a]Values based on renaturation curves. H values are obtained from non-normalized melting curves with eq 2. [b]T_M values based on the first derivative (dA/dT) of the acquired melting curves.

dx.doi.org/10.1021/ja311873t | J. Am. Chem. Soc. 2013, 135, 5399–5407

Table 2. Thermodynamics Parameters of DNA with Oxidized or Chemically Reduced DM[a]

	DNA				DNA with DM_{ox}				DNA with DM_{red}			
condition	$\Delta H°$	$\Delta S°$	$\Delta G°^{b}$	$K_a{}^{b}$ (M^{-1})	$\Delta H°$	$\Delta S°$	$\Delta G°^{b}$	$K_a{}^{b}$ (M^{-1})	$\Delta H°$	$\Delta S°$	$\Delta G°^{b}$	$K_a{}^{b}$ (M^{-1})
20mer, 5.9 mM Na^+	−119	−357	−7.6	6.4	−80	−208	−8.4	3.8×10^7	−117	−344	−7.7	2.6×10^2
40mer, 5.9 mM Na^+	−109	−313	−8.3	1.9×10^2	−62	−149	−9.1	2.5×10^7	−143	−407	−8.5	2.9×10^3
20mer, 16.5 mM Na^+	−120	−348	−7.8	5.6×10^2	−85	−217	−8.5	8.7×10^7	−120	−344	−7.9	3.0×10^3

[a]Parameters from van't Hoff analysis of renaturation curves. Units for $\Delta H°$ and $\Delta G°$ are kcal/mol, and $\Delta S°$ is in cal/mol·K. [b]$\Delta G°$ at T_M and K_a at T_{work}.

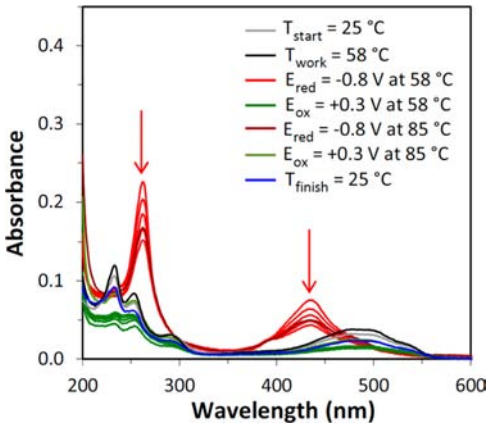

Figure 2. *In situ* UV−vis spectroelectrochemical characterization of 100 μM DM in SSC buffer (5.9 mM Na^+). Repeated switching of the DM redox states is observed as redox potentials are successively applied five times at 58 °C.

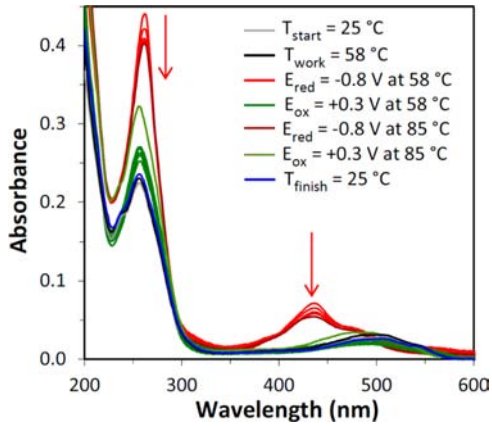

Figure 3. Demonstration of cyclic denaturation and renaturation of DNA by redox-state switching of DM: absorption spectra of complementary 20mer DNA oligonucleotides in the presence of DM (molar ratio 2:1) in SSC buffer (5.9 mM Na+) at 58 °C, detected by *in situ* UV−vis spectroelectrochemistry. A significant increase in absorbance is observed at 260 nm upon reducing DM at −0.8 V, indicating denaturation, which is reversed upon re-oxidation of DM at +0.3 V, indicating renaturation.

absorbance for re-oxidized DM may be related to further formation of quinone methide intermediates from the hydroquinone.[45,46] These intermediates result from an irreversible glycosidic cleavage of the sugar ring and were shown to occur under certain conditions, such as in anaerobic environments.[46] However, NMR spectra recorded before and after redox cycling showed that DM remains intact with no sign of such cleavage (data not shown). In addition, it is worth noting that Houée et al. showed that even at low oxygen partial pressure, *in vitro* re-oxidation of the hydroquinone is favored over the glycosidic cleavage of the sugar ring.[44,46]

Electrochemical Cycling of DNA Denaturation and Hybridization. Figure 3 shows typical *in situ* UV−vis spectroelectrochemical absorption spectra of electrochemically controlled cycles of denaturation and renaturation of complementary 20mer DNA oligonucleotides in SSC buffer (5.9 mM Na^+). The reversible interconversion between dsDNA and ssDNA was obtained by electrochemical cycling of the DM redox state at the working temperature of 58 °C. The strength in utilizing *in situ* UV−vis spectroelectrochemistry[48] lies in that the behavior of DNA and DM can be followed simultaneously. Changes in the conformational state of DNA upon the application of the switch potential were followed at 260 nm, whereas intercalation and the change in the redox state of DM were followed between 400 and 500 nm.

Upon the application of −0.8 V a characteristic peak at 435 nm appeared for reduced DM. This was accompanied by a significant hyperchromic shift at 260 nm indicating denaturation of dsDNA. Upon applying +0.3 V, the hyperchromic shift was reversed. A dramatic decrease at 260 nm was observed indicating renaturation of ssDNA and the peak for oxidized DM re-appeared at 500 nm. As the sample was heated to the heat denaturation temperature 85 °C at the end of the experiment, the 20mer DNA was in a denatured state irrespective of the DM redox state (Figure 1). Upon applying −0.8 V at 85 °C, to achieve reduction of DM, the observed hyperchromic shift at 260 nm corresponded with the shift obtained during reduction at 58 °C. This confirmed that denaturation was in fact occurring at the working temperature due to the reduction of DM. As the potential was switched to +0.3 V to achieve re-oxidation of DM, the peak for oxidized DM appeared blue-shifted at 480 nm with an increased absorbance. As shown by others, free DM exhibits a peak maximum at 480 nm, and intercalation into dsDNA results in red-shift of the peak maximum as well as a decrease in absorbance.[34,36] It could thus be concluded that oxidized DM was free at the heat denaturation temperature whereas it was intercalated at the working temperature (due to the red-shifted peak at 500 nm). Consequently, it could be established that renaturation did in fact take place upon the re-oxidation of DM. These findings corresponded well with the initial assessments on the effect of oxidized/reduced DM on DNA.

As a further control the experiment was conducted at 25 °C, a temperature where dsDNA was shown to be hybridized irrespective of the redox state (see Figure 1). As visualized in Figure S3, upon applying −0.8 V to achieve reduction of DM, a considerably smaller and less stable hyperchromic shift at 260 nm was obtained. Hence, it corroborated that the shift observed upon the reduction of DM at 58 °C (Figure 3) must have been due to the additional changes occurring in the sample affecting the absorbance. Such changes are likely to be denaturation of dsDNA, since an increase in absorbance is seen upon exposure

dx.doi.org/10.1021/ja311873t | J. Am. Chem. Soc. 2013, 135, 5399−5407

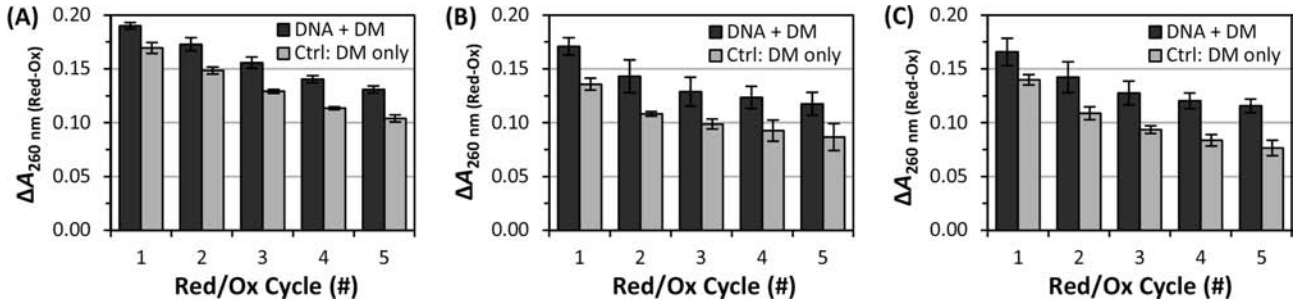

Figure 4. Comparison of $\Delta A_{260\ nm}$ for each reduction/oxidation cycle of DM only and DM in the presence of complementary (A) 20mer (SSC buffer, 5.9 mM Na^+), (B) 40mer (SSC buffer, 5.9 mM Na^+), and (C) 20mer (SSC buffer, 16.5 mM Na^+) DNA oligonucleotides. The difference is larger for DM in the presence of DNA, indicating contributions from changes in the DNA conformation. Error bars represent standard error ($n \geq 3$).

of the aromatic rings of the DNA nucleotides as dsDNA denatures into ssDNA.[3] An additional control where DM was omitted from the sample, Figure S4, confirmed that the successive application of the selected redox potentials did not induce dsDNA denaturation as no change in absorbance at 260 nm was observed. It additionally confirmed that the DNA nucleotides were not undergoing oxidation or reduction. This was substantiated by the findings of Nowicka et al. where an increase in the absorbance was observed upon the electrochemical oxidation of guanine and adenine at potentials above +0.9 V vs quasi Pt.[49] Meanwhile, others have reported more negative potentials for the reduction of nucleotides compared to the ones used in this study.[50]

Cheng et al. studied the *in vitro* effects of the electrochemical reduction of DM on fish sperm DNA to elucidate the *in vivo* cardiotoxicity of DM upon administration as a clinical drug. The authors concluded that at DNA-phosphate:DM ratios of 1:1, the DNA was damaged by fragmentation due to free radical generation upon DM reduction.[51] Hence, potential fragmentation was investigated. 20mer dsDNA, in the presence of DM, before and after redox cycling was analyzed with capillary gel electrophoresis (see Figure S5). No evidence of DNA degradation or fragmentation was found. A clear peak for a 20 bp DNA fragment was visible both before and after the redox cycling.

Electrochemically controlled DNA denaturation and renaturation was also realized for complementary 40mer DNA oligonucleotides (SSC buffer, 5.9 mM Na^+) and 20mer DNA oligonucleotides in higher salt concentration (SSC buffer, 16.5 mM Na^+). Apart from employing different working and heat denaturation temperatures (Table 1), experimental procedures were kept identical to the first condition of 20mer DNA in the lower salt concentration. Figure S6 shows the recorded UV−vis absorption spectra upon the successive application of the redox potentials. In Figure 2 it can be seen that DM absorbs in the area of 260 nm irrespective of its redox state, and thus interferes with the signal obtained for DNA at 260 nm. Therefore, the absolute difference in absorbance at 260 nm obtained from switching the redox state of DM only and DM in the presence of DNA were analyzed for each of the investigated conditions (see Figure 4). It is evident that the difference in absorbance observed upon reduction of DM only remained smaller compared to DM in the presence of DNA. Again, this confirmed that the larger difference obtained for DM in the presence of DNA was due to additional changes, such as denaturation of dsDNA, occurring in the sample.

The reproducibility of cycles of electrochemically controlled DNA denaturation and renaturation was studied by quantifying the response which could exclusively be assigned to DNA for all investigated conditions. Using eq 3, the switching in absorbance obtained exclusively from changes in the DNA conformation was acquired and is summarized in the switch diagram in Figure 5A. It can thus be confirmed that, after the subtraction of the

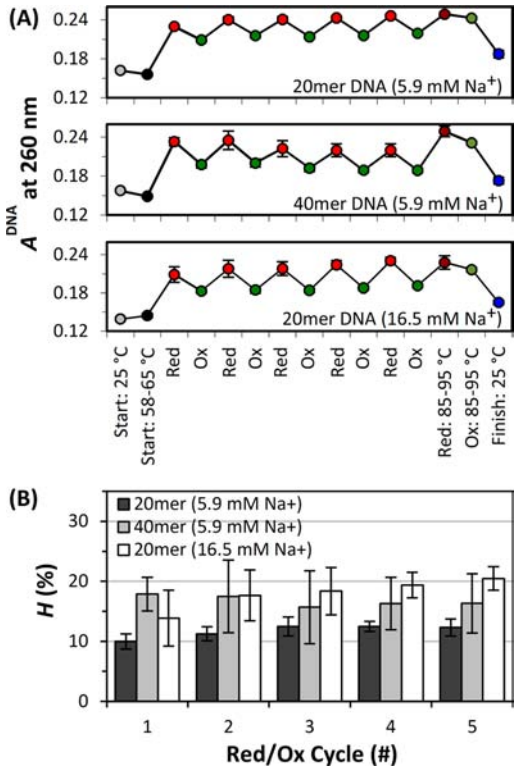

Figure 5. (A) Switch diagrams displaying the change in absorption at 260 nm caused by five consecutive cycles (144 s/cycle) of DNA denaturation (red circles) and renaturation (green circles), controlled by switching the redox state of DM, at three different experimental conditions. Signals represent the exclusive absorbance of DNA (eq 3) at the given conditions. (B) Hyperchromic shifts per reduction/oxidation cycle, to quantify the efficiency of electrochemical control of hybridization. Error bars represent standard errors ($n \geq 3$).

contribution of DM absorbance at 260 nm, a clear stable switching signal remained which arises from the electrochemically controlled DNA denaturation and renaturation cycles. A similar switching behavior was observed across all three studied conditions, with the best reproducibility for the 20mer dsDNA in low salt concentration (standard error of absorbance within ±0.003) and a slight drift in the signal when increasing the

dx.doi.org/10.1021/ja311873t | J. Am. Chem. Soc. 2013, 135, 5399−5407

length of the oligonucleotide (40mer). The hyperchromic shifts obtained for each of the five reduction/oxidation cycles were calculated using eq 4 and are presented in Figure 5B. For the electrochemical control of hybridization, hyperchromic shifts below 20% were achieved. This corresponded to 57−80% of the total DNA being electrochemically controlled as compared to control by thermal means. This may be related to the incomplete renaturation of DNA as a result of the used salt concentration. Conducting the experiment at a higher salt concentration resulted in a more complete renaturation of DNA (lower relative $A_{260\ nm}$ values) compared to the lower salt concentration of 5.9 mM Na^+ (Figure 5), which was initially chosen to favor denaturation. In the prevailing model for this process, the counterion condensation theory,[52,53] the free energy is formed in the limit of an infinitely long charged polymer. Contributions to the free energy arise from a sum of Debye−Hückel interactions of counterions with a charged polymer plus entropy of mixing terms. That is, the population of condensed counterions is, in the dilute regime, not determined by the bulk salt concentration but rather by the linear charge density of the polymer and the counterion valence. Assuming that the limiting conditions of the model apply to the present system, the results in this study suggest therefore that solvent entropy contributions, arising from counterion redistribution at the duplex/single-strand transition, is responsible for the observed effects on the renaturation efficiency of the DNA.[4,52,53] However, a fuller quantitative exploration is warranted. Another possible reason may be related to the working temperature. By selecting a working temperature where 100% of the DNA was in a denatured state in the presence of reduced DM, it was not feasible to avoid slight denaturation of the DNA in the presence of oxidized DM (Figure 1 and Figure S1).

To validate the results observed with *in situ* UV−vis spectroelectrochemistry using an independent method, the same electrochemical switch experiments were repeated employing *in situ* CD spectroelectrochemistry. Initially, as seen in Figure S7A, the change in CD upon denaturation of dsDNA was investigated by end-point measurements at 25 and 85 °C. At 25 °C when renatured, complementary 20mer DNA oligonucleotides in SSC buffer (5.9 mM Na^+) displayed a strong positive band at 275 nm, while a strong negative band was obtained at 250 nm which is in agreement with previous findings in the literature.[54] Upon denaturation at 85 °C, bands at 250 and 275 nm decreased as observed before.[55] Figure S7B shows the CD spectra of complementary 20mer DNA oligonucleotides in the presence of oxidized DM. When renatured at 25 °C, a strong positive band at 275 nm was found with a dip observed at 250 nm and a strong negative band at 300 nm. These observations were also made by Dalgleish et al. on the characterization of DM intercalated in dsDNA at various concentrations.[56] Upon denaturation at 85 °C, bands at 275 and 300 nm decreased. Due to the decrease in the CD signal at 275 nm upon denaturation of DNA in the absence and presence of oxidized DM, this signal was monitored in the electrochemical switch experiments.

Figure 6A shows the *in situ* CD spectroelectrochemical spectra for DNA denaturation and renaturation cycles driven by electrochemically switching the redox state of DM under identical experimental conditions and procedures as used for the *in situ* UV−vis spectroelectrochemical measurements (Figure 3). The CD spectra were collected at a high scan speed and low response time on the sacrifice of resolution but

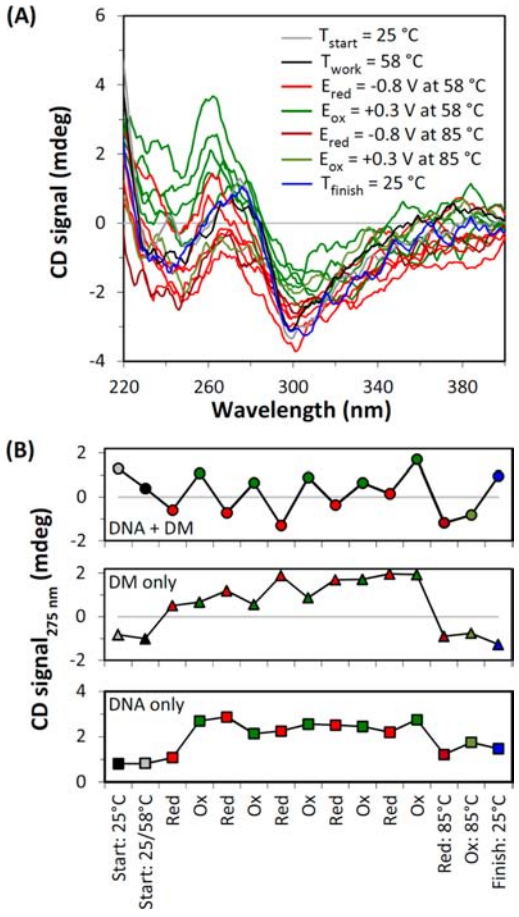

Figure 6. Validation of electrochemically controlled DNA denaturation and renaturation cycles with *in situ* CD spectroelectrochemistry. (A) CD spectra of complementary 20mer DNA oligonucleotides in the presence of DM (molar ratio 2:1) in SSC buffer (5.9 mM Na^+) at 58 °C. Consistent change in CD of the DNA is observed at 275 nm upon switching the redox state of DM by cycling −0.8 and +0.3 V. (B) Switch diagram of change in $CD_{275\ nm}$ for dsDNA in the presence of DM and controls DM only and dsDNA only. Consistent switching, upon cycling −0.8 and +0.3 V, is only seen for DNA in the presence of DM.

gain of experimental stability.[57] Interestingly, also here, a consistent switching in CD was clearly observed upon the successive cycling of the redox potentials. As the sample was heated to the final heat denaturation temperature of 85 °C, the observed spectrum of denatured DNA corresponded well with the spectra obtained at the working temperature during the phase of reduced DM. To make this observation clearly visible, the CD signals were depicted at the relevant wavelength (275 nm) of the sample along with two controls (see Figure 6B). Whereas a clear switching of the CD signal was observed for DNA in the presence of DM, no switching was observed for the controls. It can be seen that upon reduction of DM, the CD at 275 nm for DNA decreased correspondingly to changes seen for thermal melting of DNA in the presence of DM (Figure S7B). We therefore concluded that the observed conformational changes of the DNA are due to denaturation events, and that the proof-of-principle for our proposed technique was confirmed with a second independent method. At present, the underlying reasons for the observed effects induced by oxidized/reduced DM are not fully understood. To understand the system in detail, further investigation is needed, for example

dx.doi.org/10.1021/ja311873t | *J. Am. Chem. Soc.* 2013, 135, 5399−5407

using molecular dynamics modeling. However, following the available literature and theoretical consideration we are confident that a plausible reason for the observed electrochemical denaturation is related to the protonation state of the reduced DM. Kano et al. determined the pK_a values for adsorbed oxidized and reduced Adriamycin (AM) on a mercury electrode as 8.53 and 6.83.[58] AM structurally differs to DM only by one extra hydroxyl group at position C14. The pK_a values of oxidized AM were found to correspond well to oxidized DM.[47] Consequently, it may be inferred that the reduced DM behaves similar to reduced AM and thus is partially deprotonated at neutral pH. Due to electrostatic repulsion forces from the negatively charged DNA, this may facilitate de-intercalation of DM. If a working temperature was chosen where hybridization can only be achieved by duplex stabilization through the intercalating DM, reduction of DM would result in denaturation of the dsDNA. This consideration is exactly matched by our experimental observations. However, it is worth noting that a study by Jones and Wilson[59] showed that pK_a values of ligands, here the ethidium bromide analogue 3,8-diamino-6-phenyl-phenanthridine, shift as a function of the ionic strength upon binding to DNA. This may have an important impact on the understanding of the system.

We believe that the concept presented here and the successful proof-of-concept have significant translational importance. It addresses one of the most significant road blocks in the development of decentralized molecular testing associated with the need to control cycles of large intervals or prolonged periods of elevated solution temperatures to enable, for example, nucleic acid amplification by control of hybridization. However, in the present study, based on the T_M values of the DNA oligonucleotides that were used, the temperature was kept constant at around 60 °C during the denaturation/renaturation cycles. Decreasing this working temperature will render the method further economical in terms of energy consumption. Additionally, while the system has been shown to work for short oligonucleotides, future experiments will have to address the challenge of longer oligonucleotides that have higher T_M values which, in the current system, would lead to higher working temperatures. While they are expected to be lower than the maximum denaturation temperatures used in standard nucleic acid amplification protocols (normally ∼95 °C), this will nevertheless be relevant for the application of the system. Lastly, compared to, for example, standard PCR protocols, the denaturation/renaturation cycle time of 144 s is quite long. However, if compared to other electrochemical approaches[6] for controlling reversible DNA hybridization, the method presented here is about twice as fast already. Furthermore, many conventional biomolecular techniques rely on buffered solutions to achieve the optimum performance of various components, such as enzymes[60] or fluorescent labels.[61] Dramatic changes for example in pH or temperature may easily impede their performance. In contrast to other studies,[6] no dramatic changes in the composition of the solution was required to achieve electrochemical control of DNA denaturation/renaturation, thus, demonstrating the feasibility of the method in this study in buffered media. Additionally, no degradation of DNA was detected.

CONCLUSION

We have demonstrated the proof-of-principle of a new electrochemical method to control reversible DNA hybridization as an alternative to heating and cooling of reaction solutions. The system was thoroughly investigated using three experimental conditions and two independent analysis techniques. At present, the method in this study is slower than conventional methods for controlling reversible DNA hybridization, however isothermal and no extreme chemical conditions are inflicted. Because it is based on electrochemical redox-state switching of its active ingredient, the method has an immense potential to greatly simplify developments of miniaturized molecular diagnostic analysis systems.

ASSOCIATED CONTENT

Supporting Information

Sequence information; experimental procedures for CD; melting curves and spectra from switch experiments for further conditions and controls; end-point melting measurements with CD. This material is available free of charge via the Internet at http://pubs.acs.org.

AUTHOR INFORMATION

Corresponding Author

till.bachmann@ed.ac.uk

Notes

The authors declare no competing financial interest.

ACKNOWLEDGMENTS

This work was jointly funded by the School of Biomedical Sciences and the School of Physics and Astronomy of the University of Edinburgh. We acknowledge Janice Bramham who helped us with the CD experiments carried out at the Edinburgh Biophysical Characterization Facility, supported by SULSA, BBSRC, and the Wellcome Trust.

REFERENCES

(1) Yakovchuk, P.; Protozanov, E.; Frank-Kamenetskii, M. D. *Nucleic Acids Res.* **2006**, *34*, 564.
(2) Kool, E. T. *Annu. Rev. Biophys. Biomol. Struct.* **2001**, *30*, 1.
(3) Mergny, J.-L.; Lacroix, L. *Oligonucleotides* **2003**, *13*, 515.
(4) Owczarzy, R.; You, Y.; Moreira, B. G.; Manthey, J. A.; Huang, L.; Behlke, M. A.; Walder, J. A. *Biochemistry* **2004**, *43*, 3537.
(5) Ageno, M.; Dore, E.; Frontali, C. *Biophys. J.* **1969**, *9*, 1281.
(6) Wang, Y.-C.; Lin, C.-B.; Su, J.-J.; Ru, Y.-M.; Wu, Q.; Chen, Z.-B.; Mao, B.-W.; Tian, Z.-W. *Anal. Chem.* **2011**, *83*, 4930.
(7) Hutton, J. R. *Nucleic Acids Res.* **1977**, *4*, 3537.
(8) Drummond, T. G.; Hill, M. G.; Barton, J. K. *Nat. Biotechnol.* **2003**, *21*, 1192.
(9) Gebala, M.; Stoica, L.; Neugebauer, S.; Schuhmann, W. *Electroanal.* **2009**, *21*, 325.
(10) Bier, F. F.; von Nickisch-Rosenegk, M.; Ehrentreich-Förster, E.; Reiss, E.; Henkel, J.; Strehlow, R.; Andresen, D. *Adv. Biochem. Eng./Biotechnol.* **2008**, *109*, 433.
(11) Leinberger, D. M.; Grimm, V.; Rubtsova, M.; Weile, J.; Schröppel, K.; Thomas, A.; Wichelhaus, T. A.; Knabbe, C.; Schmid, R. D.; Bachmann, T. T. *J. Clin. Microbiol.* **2010**, *48*, 460.
(12) Saiki, R. K.; Gelfand, D. H.; Stoffel, S.; Scharf, S. L.; Higuchi, R.; Horn, G. T.; Mullis, K. B.; Erlich, H. A. *Science* **1988**, *239*, 487.
(13) Craw, P.; Balachandran, W. *Lab Chip* **2012**, *12*, 2469.
(14) Wiedman, M.; Wilson, W.; Czajka, J.; Luo, J.; Barany, F.; Batt, A. *PCR Methods Appl.* **1994**, *3*, S51.
(15) Metzker, M. L. *Nature Rev. Genet.* **2010**, *11*, 31.
(16) Resendiz, M. J. E.; Schön, A.; Freire, E.; Greenberg, M. M. *J. Am. Chem. Soc.* **2012**, *134*, 12478.
(17) Dohno, C.; Uno, S.-N.; Nakatani, K. *J. Am. Chem. Soc.* **2007**, *129*, 11898.
(18) Lee, S. J.; Lee, S. Y. *Appl. Microbiol. Biotechnol.* **2004**, *64*, 289.
(19) Asiello, P. J.; Baeumner, A. J. *Lab Chip* **2011**, *11*, 1420.

(20) Weigl, B.; Domingo, G.; LaBarre, P.; Gerlach, J. *Lab Chip* **2008**, *8*, 1999.
(21) Holland, C. A.; Kiechle, F. L. *Curr. Opin. Microbiol.* **2005**, *8*, 504.
(22) Yager, P.; Edwards, T.; Helton, K.; Nelson, K.; Tam, M. R.; Weigl, B. H. *Nature* **2006**, *442*, 412.
(23) Zhang, C.; Xing, D. *Nucleic Acids Res.* **2007**, *35*, 4223.
(24) Luo, X.; Hsing, I.-M. *Analyst* **2009**, *134*, 1957.
(25) Wang, J. *Biosens. Bioelectron.* **2006**, *21*, 1887.
(26) Asanuma, H.; Liang, X.; Yoshida, T.; Komiyama, M. *ChemBioChem* **2001**, *2*, 39.
(27) Hamad-Schifferli, K.; Schwartz, J. J.; Santos, A. T.; Zhang, S.; Jacobson, J. M. *Nature* **2002**, *415*, 152.
(28) Ihmels, H.; Otto, D. *Top. Curr. Chem.* **2005**, *258*, 161.
(29) Erdem, A.; Kerman, K.; Meric, B.; Ozsoz, M. *Electroanal.* **2001**, *13*, 219.
(30) Deféver, T.; Druent, M.; Evrard, D.; Marchal, D.; Limoges, B. *Anal. Chem.* **2011**, *83*, 1815.
(31) Marazza, G.; Chiti, G.; Mascini, M.; Anichini, M. *Clin. Chem.* **2000**, *46*, 31.
(32) Quigley, G. J.; Wang, A. H.-J.; Ughetto, G.; van der Marel, G.; van Boom, J. H.; Rich, A. *Proc. Natl. Acad. Sci. U.S.A.* **1980**, *77*, 7204.
(33) Guin, P. S.; Das, S.; Mandal, P. C. *Int. J. Electrochem.* **2011**, *2011*, 1.
(34) Chaires, J. B.; Dattagupta, N.; Crothers, D. M. *Biochemistry* **1982**, *21*, 3933.
(35) Lin, P.-H.; Kao, Y.-H.; Chang, Y.; Cheng, Y.-C.; Chien, C.-C.; Chen, W.-Y. *Biotechnol. J.* **2010**, *5*, 1.
(36) Chu, X.; Shen, G.-I.; Jiang, J.-H.; Kang, T.-F.; Xiong, B.; Yu, R.-Q. *Anal. Chim. Acta* **1998**, *373*, 29.
(37) Wilhelm, M.; Mukherjee, A.; Bouvier, B.; Zakrzewska, K.; Hynes, J. T.; Lavery, R. *J. Am. Chem. Soc.* **2012**, *134*, 8588.
(38) Puglisi, J. D.; Tinoco, I. J. *Methods Enzymol.* **1989**, *180*, 304.
(39) Breslaur, K. J.; Sturtevant, J. M.; Tinoco, I. J. *J. Mol. Biol.* **1975**, *99*, 549.
(40) IDT Biophysics. http://biophysics.idtdna.com (accessed Nov 23, 2012).
(41) Belozerova, I.; Levicky, R. *J. Am. Chem. Soc.* **2012**, *134*, 18667.
(42) Ibrahim, M. S. *Anal. Chim. Acta* **2001**, *443*, 63.
(43) Neudeck, A.; Marken, F.; Compton, R. G. *Electroanalytical Methods: Guide to Experiments and Applications*, 2nd ed.; Scholz, F., Ed.; Springer Verlag: Berlin-Heidelberg, 2010; p 188.
(44) Houée-Levin, C.; Gardés-Albert, M.; Ferradini, C. J. *Free Radic. Biol. Med.* **1986**, *2*, 89.
(45) Kleyer, D. L.; Koch, T. H. *J. Am. Chem. Soc.* **1984**, *106*, 2380.
(46) Abdella, R. J.; Fisher, J. *Environ. Health Perspect.* **1985**, *64*, 3.
(47) Bouma, J.; Beijnen, J. H.; Bult, A.; Underberg, W. J. M. *Pharm. Weekblad, Sci. Ed.* **1986**, *8*, 109.
(48) Shi, Y.; Slaterbeck, A. F.; Sleiskar, C. J.; Heineman, W. R. *Anal. Chem.* **1997**, *69*, 3679.
(49) Nowicka, A. M.; Zabost, E.; Donten, M.; Mazerska, Z.; Stojek, Z. *Bioelectrochemistry* **2007**, *40*, 440.
(50) Fojta, M. *Electroanal.* **2002**, *14*, 1449.
(51) Cheng, G.; Qu, H.; Zhang, D.; Zhang, J.; He, P.; Fang, Y. *J. Pharma. Biomed. Anal.* **2002**, *29*, 361.
(52) Record, M. T., Jr.; Anderson, C. F.; Lohman, T. M. *Q. Rev. Biophys.* **1978**, *2*, 103.
(53) Manning, G. S. *Biophys. Chem.* **2002**, *101*−*102*, 461.
(54) Bishop, G. R.; Chaires, J. B. *Curr. Protoc. Nucleic Acid Chem.* **2002**, 11:7.11.1−7.11.8.
(55) Baase, W. A.; Johnson, W. C., Jr. *Nucleic Acids Res.* **1979**, *6*, 797.
(56) Dalgleish, D. G.; Fey, G.; Kersten, W. *Biopolymers* **1974**, *13*, 1757.
(57) Garbett, N. C.; Ragazzon, P. A.; Chaires, J. B. *Nat. Protoc.* **2007**, *2*, 3166.
(58) Kano, K.; Konse, T.; Kubota, T. *Bull. Chem. Soc. Jpn.* **1985**, *58*, 424.
(59) Jones, R. L.; Wilson, D. *Biopolymers* **1981**, *20*, 141.
(60) Cline, J.; Braman, J. C.; Hogrefe, H. H. *Nucleic Acids Res.* **1996**, *24*, 3546.
(61) You, Y.; Tataurov, A. V.; Owczarzy, R. *Biopolymers* **2011**, *95*, 472.